InGaAsP photonic crystal slot nanobeam waveguides for refractive index sensing

Bowen Wang[1, 2, a], Mehmet A. Dündar[1], Richard Nötzel[1], Fouad Karouta[1§], Sailing He[2] and Rob W. van der Heijden[1]
[1]COBRA Research Institute, Eindhoven University of Technology, P.O. Box 513, NL-5600 MB Eindhoven, The Netherlands
[2] Centre for Optical and Electromagnetic Research, JORCEP [KTH-ZJU Joint Research Center of Photonics], Zijingang Campus, Zhejiang University, Hangzhou 310058, China

ABSTRACT

Results are presented on the use of InGaAsP photonic crystal nanobeam slot waveguides for refractive index sensing. These sensors are read remote-optically through photoluminescence, which is generated by built-in InGaAs quantum dots. The nanobeams are designed to maximize the electromagnetic field intensity in the slot region, which resulted in record-high sensitivities in the order of 700 nm/RIU (refractive index unit). A cavity, created by locally deflecting the two beams towards each other through overetching, is shown to improve the sensitivity by about 20%.

Keywords: photonic crystal, slot, nanobeam

1. INTRODUCTION

Progress made in the miniaturization of fluidic circuits has led to the emerging field of optofluidics, which is the merging of photonic circuits with micro- or nanofluidic circuits[1-3]. The porous nature of a photonic crystal (PhC) nanocavity, consisting of patterns of etched holes, makes it naturally very suitable for immersion with a target fluid, while its sensitivity is large enough to detect single (bio)molecules. Nowadays, many groups all over the world work on PhC sensors, in the Si[4-10] as well as in the III-V semiconductor platform for GaAs[11, 12], InP[13, 14] or others.

A relatively new type of PhC device is the nanobeam. In this device, light is confined in two directions by total internal reflection (TIR), while in the third direction the light is manipulated by nanostructuring the beam with a one-dimensional pattern of holes[10, 15-19]. Cavities with high quality (Q) factor and small modal volumes have been made using single nanobeams[15, 16]. Since these one-dimensional devices rely on TIR in two rather than in one direction, they are more versatile than their planar PhC counterparts. Therefore, they can be made not only of conventional high-refractive index dielectrics like Si[10, 15, 17, 18], but also of relatively low-index materials as SiN_x[19] or even SiO_2[16] for high-Q devices.

A special type of nanobeam device is the double bar structure, consisting of two coupled nanobeams. The slot in between can be exploited to tune the modes[10, 17, 18] or to create a novel type of optomechanical cavity[19]. All of these structures were made in passive dielectrics as Si[10, 15, 17, 18], SiO_2 or SiN_x. Very recently, single nanobeams made in III-V semiconductors are fabricated to achieve lasing[20, 21]. In all these structures, the cavities are made by tapering the region around the defect area, such as changing the lattice constant, or by modifying the radius of the holes and

[a] Wang.Bowen@tue.nl

§ is now with the Research School of Physics & Engineering, Australian National University, Canberra, Australia

Photonic and Phononic Properties of Engineered Nanostructures, edited by Ali Adibi, Shawn-Yu Lin, Axel Scherer,
Proc. of SPIE Vol. 7946, 79461C · © 2011 SPIE · CCC code: 0277-786X/11/$18 · doi: 10.1117/12.873709

the distance between the holes. In addition, because of the strong optical field that exists in the slot region[6, 22], these devices are promising to have applications in sensing.

In this work, InGaAsP PhC slot nanobeam waveguides consisting of two parallel suspended beams separated by a small gap are investigated. Each beam is patterned with a one-dimensional (1D) line of holes. InAs quantum dots (QDs) are embedded inside the structures to generate photoluminescence. Such a structure exhibits a resonance near its band edge frequency where the group velocity is near zero. No further modification is made to form a local cavity. By measuring the resonant wavelength for different analytes, we found a high sensitivity $S = \Delta\lambda / \Delta n$ of $7 \cdot 10^2$ nm/RIU (refractive index unit)[23]. For another structure with a cavity, a sensitivity of $9 \cdot 10^2$ nm/RIU is achieved. These record high values for S correspond directly to the large overlap of the mode field with the analyte[24], particularly in the slot region. Structures based on luminescent III-V semiconductors are attractive as they offer the full on-chip integration with sources, or the operation as lasers to increase the refractive index resolution[13]. In addition, it can be employed using remote readout, not requiring the delicate attachment of optical fibers or electrical wiring.

2. SIMULATION

A PhC slot nanobeam slow light waveguide was designed by using MIT photonic bands software package (MPB)[25] and three-dimensional finite-difference time-domain method[26]. The top view and cross sectional view of the unit cell of waveguide used in the bandstructure calculation is shown in Fig. 1(a) and (b), respectively. The waveguide is defined by the lattice constant (490 nm), width of single nanobeam (450 nm), width of the slot area (200 nm), distance between the symmetric holes (650 nm), diameter of the holes (310 nm) and the thickness of the membrane (220 nm). Since the nanobeam is used as a liquid sensor, the environment refractive index is set to 1.333 in the bandstructure calculation from MPB, corresponding to water. The bandstructure is displayed in Fig. 1 (c). There are four bands under the light cone of water, whose cutoff wavelengths are at 1706.8 nm ($\omega a/2\pi c$=0.2871), 1631.5 nm ($\omega a/2\pi c$=0.3003), 1404.7 nm ($\omega a/2\pi c$=0.3488) and 1336.9 nm ($\omega a/2\pi c$=0.3665), respectively. The intensity distributions of four band-edge modes in the central plane of the unit cell are shown in the inset of Fig. 1(c). For the band-edge mode of the third band, the light is strongly localized inside the slot region and holes. This mode is referred to as slot mode. The slot mode has most of its energy within the environment, rather than in the semiconductor, so it is sensitive to the environment change. The slot mode profile of this waveguide is similar to the even mode profile around cavities in coupled nanobeams as described in Ref. [10, 17, 18] but is not the same, which will be discussed later. To make a real sample, the waveguide should be cut off, which means the length of waveguides is always finite. Additionally there is a constraint on the length of these waveguides because they need to be able to support their own weight and not collapse in the fabrication and processing. A PhC slot nanobeam slow light waveguide with 27 periods was designed. In our simulation, the slot modes of the cavity infiltrated with distilled water (n=1.333) and sugar/water solution (n=1.3417) are at 1416.5 nm and 1422.8 nm respectively, with Q factors of 2000. By relating the peak position change with the change of refractive index, we obtain an impressive sensitivity value of 724 nm/RIU. Because the structure is finite, losses occur near the two ends. To decrease these losses, additional PhC mirrors with lattice constant of 490 nm and hole diameter of 400 nm were added, which increased the calculated Q factors to 3000. The electrical field (E_y) profile and the intensity distribution of the slot mode of the finite waveguide with the extra mirrors infiltrated with distilled water in the central plane are presented in Fig. 1(d) and (e), respectively. The light is strongly localized in the central part of PhC slot nanobeam slow light waveguide. The light localization of the band edge mode in the central part of our 1D finite length waveguide is analogous to the light localization of band edge modes in finite two dimensional photonic crystals in Ref. [27]. Comparing with the even mode in the coupled nanobeams cavity [cf. Fig. 2 in Ref. 17] where the light is localized in the slot region but also in the semiconductor, our slot mode has more light confined in the low refractive index region, i.e., in the slot region but also in the holes.

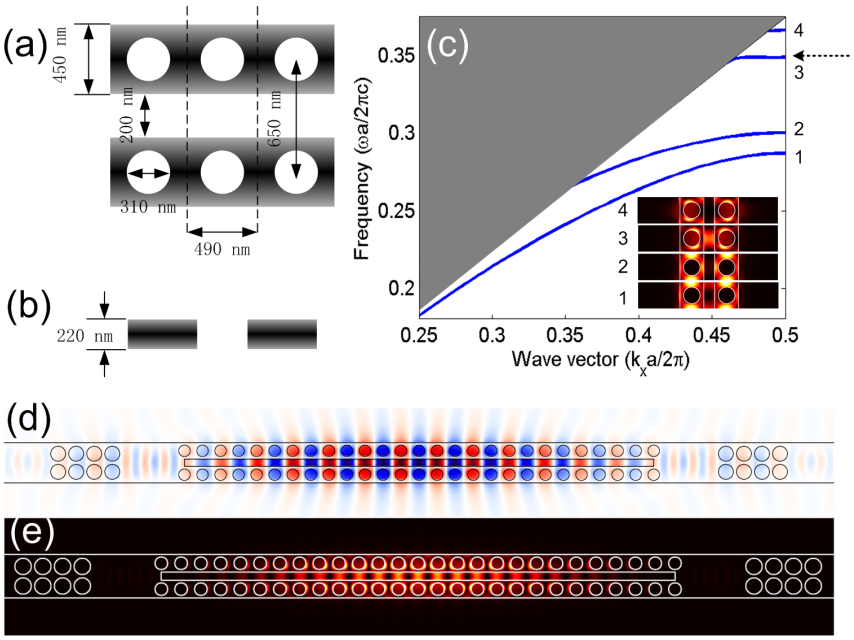

Fig. 1 Schematic sketch of a PhC slot nanobeam slow light waveguide from (a) top view, (b) cross-sectional view. A unit cell is marked by two dashed lines. (c) Band structure of the waveguide. The gray region is the light cone of water. The inset shows the intensity distributions of four band-edge modes in the central plane from bottom to top accordingly. (d) The electrical field (E_y) profile and (e) the intensity distribution of the slot mode of a finite waveguide with some extra mirrors infiltrated with distilled water in the central plane.

3. FABRICATION

An InGaAsP PhC slot nanobeam slow light waveguide was fabricated on a 220 nm thick InGaAsP membrane which contains a single layer of self-assembled InAs QDs (density 3×10^{10} cm^{-2})[28]. The pattern was defined by high resolution Electron Beam Lithography on a 350 nm thick ZEP 520A resist and subsequently transferred to an underlying 400 nm thick SiNx mask layer by Reactive Ion Etching. Next, the pattern was etched in an InP-InGaAsP-InP layer stack, by Inductively Coupled Plasma etching using $Cl_2/Ar/H_2$ chemistry. Finally, a free standing InGaAsP membrane is achieved by selective wet chemical etching of InP using an $HCl:H_2O$=4:1 solution at 2 °C. Because for high sensitivity the nanobeams have strong requirements on the hole size and beam widths, they tend to be very fragile. These specifications are met by carefully adjusting the dose factors for the Electron Beam Lithography. We used SiN_x first to obtain the dose factors for the nanobeam with the correct parameters. Fig. 2(a) shows the Scanning Electron Microscope (SEM) image of a failed sample, which is not underetched. Fig. 2(b) shows the SEM image of a suspended nanobeam, in which both the diameter of the holes are smaller than what we want. Fig. 3(c) shows the SEM image, in which the parameters of the structure are good. Then with the proper dose factors found for the SiN_x mask, the structures were transferred to InGaAsP. Fig. 2(d) shows the SEM image of part of an array of InGaAsP slot PhC nanobeam slow light waveguides with the designed parameters, where the waveguide length was varied. Analyte was placed on the top of the sample from a pipette. This entirely immerses the nanobeam structure with the liquid. Then a 0.15 mm thick cover glass was placed on the filled sample in order to avoid water evaporation and to achieve a flat and constant thickness layer of analyte on top of the sample. Since excess fluid is present, not only the holes, but also the top of the sample and under-etched void is filled with the liquid. Because of the incorporated QDs, a photoluminescence (PL) experiment can be conducted easily by using a continuous wave CW diode laser (λ=660 nm) as an excitation source. An optical microscope objective with NA=0.5 and magnification of 50 is used for both excitation of the cavities and collection of the PL. After dispersing the PL in a 50 cm focal length monochromator, the collected signal is detected by a liquid nitrogen cooled InGaAs camera.

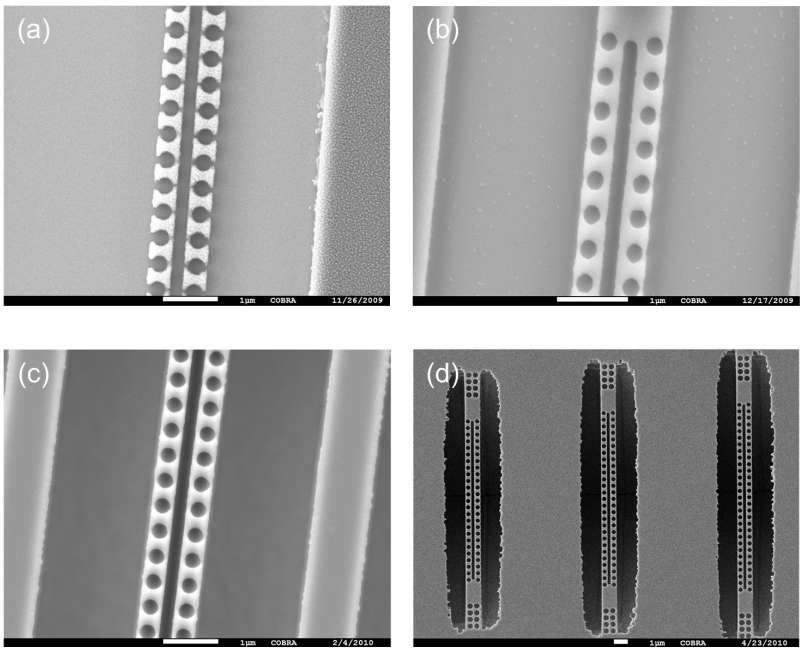

Fig. 2 SEM images of (a) a failed sample with SiN, (b) a suspended SiN nanobeam, (c) a good SiN nanobeam and (d) the InGaAsP slot PhC nanobeam slow light waveguide with the designed parameters.

4. MEASUREMENT AND DISCUSSION

In order to measure the sensitivity of our structure, the sample was infiltrated with distilled water and sugar/water solution. The refractive indices of distilled water and sugar/water solution are 1.333 and 1.342, respectively, which can be found in Ref. 29. The PL spectrum of the InGaAsP slot PhC nanobeam slow light waveguide with the infiltration of distilled water is shown in Fig. 3(a). There is a peak at 1386.5 nm which is the slot mode, with a Q factor of 500. Fig. 3(b) shows the PL spectrum of the same waveguide with the infiltration of sugar/water solution. The peak redshifts to 1392.4 nm. The difference of the peak position gives a sensitivity of $7 \cdot 10^2$ nm /RIU, which has been confirmed several times later. A sensitivity close to the predicted value of 724 nm/RIU, implies that the calculated mode pattern agrees with experiment. Previously people locally probed the EM field distribution by a scanning near-field optical microscopy experiment to measure the high intensity in a different slot structure[10]. In the present work we probe it directly by a sensitivity experiment as previously demonstrated[24]. After improving the Q factor the structure is promising for application, while the Q factor can be improved by introducing a better mirror just on the ends of the slot region[27]. The slight discrepancy between simulation and experiment of the peak position, Q factor and sensitivity can be attributed to several effects, including the uncertainty of the membrane thickness after an O_2 plasma and H_3PO_4 etch before the infiltration of solvents, and the roughness in the slot region which weakens the localization of the light inside the slot region.

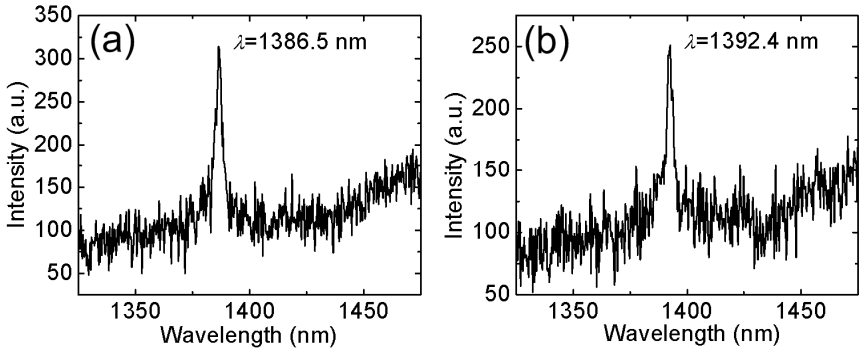

Fig. 3 PL spectrum of the waveguide with the infiltration of (a) distilled water (n=1.333) and (b) sugar/water solution (n=1.342).

Because of the over etching of one device caused change in device geometry, we also have an InGaAsP PhC slot nanobeam slow light waveguide with stuck nanobeams, which is shown in Fig. 4(a). In this device, the parameters are the same as those we mention above, except for the hole diameter, which is increased to 330 nm. However, for this waveguide, the nanobeams bend inward which makes the slot region narrow in the central part and a cavity is formed. The bend may be due to the weak wall because of the larger hole diameter. The sensitivity of this structure is measured in the same way used before. Fig. 4(b) shows the PL spectrum of the cavity with the infiltration of distilled water. The peak at 1502.2 nm is the slot cavity mode, with a Q factor of 700. Fig. 3(d) shows the PL spectrum of the same structure with the infiltration of sugar/water solution. The peak has a redshift of 8.1 nm. This gives a sensitivity of about $9 \cdot 10^2$ nm/RIU. Compared to the normal waveguide, the resonant wavelength shows a big red shift about 100 nm, while this cavity has a higher sensitivity and a higher Q factor. The reason of the red shift of the resonant wavelength is the decrease of the separation between the two nanobeams[17,18]. We have also modeled the bend case in our simulation, and found that the slot modes of the cavity infiltrated with distilled water (n=1.333) and sugar/water solution (n=1.3417) are at 1477.0 nm and 1482.6 nm respectively, which gives a sensitivity of 643 nm/RIU. The intensity distribution of the slot mode of the cavity type waveguide infiltrated with distilled water in the central plane is presented in Fig. 3(d). The light is still strongly localized in the slot region. The difference between the experiment and simulation results is caused by parameters uncertainty as inferred from SEM image. The higher sensitivity in the experiment may be also caused by the larger hole size in the bend structure.

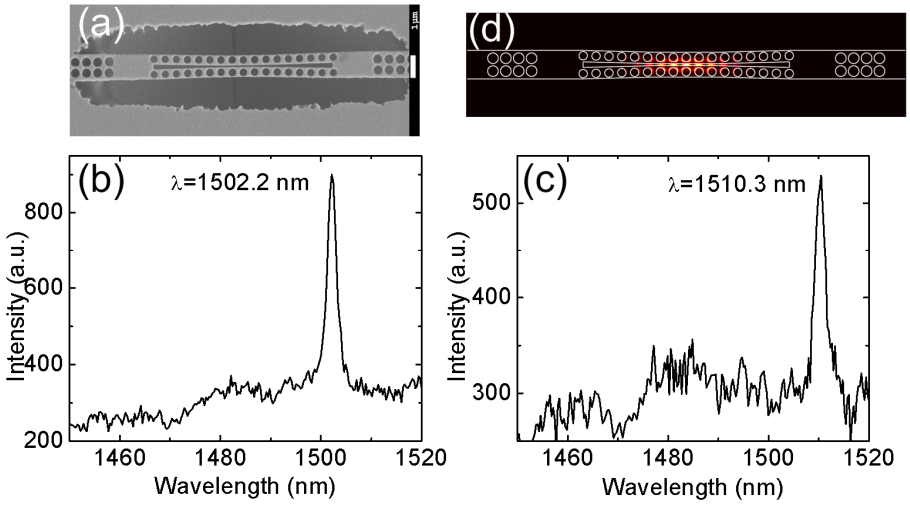

Fig. 4 (a) SEM image of a cavity type InGaAsP PhC slot nanobeam slow light waveguide; PL spectrum of the cavity type waveguide with the infiltration of (b) distilled water (n=1.333), (c) sugar/water solution (n=1.342); (d) The field intensity distribution for the slot mode of the cavity type waveguide infiltrated with distilled water in the central plane.

5. CONCLUSION

In conclusion, we presented the sensitivity to the refractive index changes of the analyte of InGaAsP PhC slot nanobeam slow light waveguides as a measure of the intensity distribution in the low index region, particularly the slot region. A high sensitivity of $7 \cdot 10^2$ nm /RIU and for a normal structure and a higher sensitivity of $9 \cdot 10^2$ nm/RIU for a cavity type structure are reported here. By introducing a real cavity into the waveguide, we believe that the *Q* factor could be increased by a few orders of magnitude[17, 19] and a very high refractive index resolution could be achieved.

6. ACKNOWLEDGEMENTS

B. Wang thanks Dr. Yaocheng Shi for useful discussion. The authors acknowledge E. J. Geluk, P. J. van Veldhoven, B. Smalbrugge and T. de Vries for their help in the fabrication processes the support from the BrainBridge project (ZJU-TU/e and Philips Research collaboration), AOARD, and the National Natural Science Foundation of China (grant 60907018).

REFERENCES

[1] Psaltis, D. S., Quake, R. and Yang, C. H., "Developing optofluidic technology through the fusion of microfluidics and optics," Nature 442, 381 (2006).

[2] Monat, C., Domachuk, P. and Eggleton, B. J., "Integrated optofluidics: A new river of light," Nature Photonics 1, 106 (2007).

[3] Erickson, D., "Special issue on 'Optofluidics',", Microfluidics and Nanofluidics. 4, 1 (2008).

[4] Chow, E., Grot, A., Mirkarimi, L. W., Sigalas, M. and Girolami, G., "Ultracompact biochemical sensor built with two-dimensional photonic crystal microcavity," Opt. Lett. 29, 1093 (2004).

[5] Lee, M. and Fauchet, P. M., "Two-dimensional silicon photonic crystal based biosensing platform for protein detection," Opt. Express 15, 4530 (2007).

[6] Di Falco, A., O'Faolain, L. and Krauss, T. F., "Chemical sensing in slotted photonic crystal heterostructure cavities," Appl. Phys. Lett. 94, 063503 (2009).

[7] Dorfner, D., Zabel, T., Hürlimann, T., Hauke, N., Frandsen, L., Rant, U., Abstreiter G. and Finley, J., "Photonic crystal nanostructures for optical biosensing applications," Biosensors and Bioelectronics 24, 3688 (2009).

[8] Skivesen, N., Têtu, A., Kristensen, M., Kjems, J., Frandsen, L. H. and Borel, P. I. "Photonic-crystal waveguide biosensor," Opt. Express 15, 3169 (2007).

[9] Mortensen, N. A., Ziao, S. and Pedersen, J., "Liquid-infiltrated photonic crystals: enhanced light-matter interactions for lab-on-a-chip applications," Microfluidics and Nanofluidics. 4, 117 (2007).

[10] Foubert, K., Lalouat, L., Cluzel, B., Picard, E., Peyrade, D., de Fornel, F. and Hadji, E., "An air-slotted nanoresonator relying on coupled high Q small V Fabry–Perot nanocavities," Appl. Phys. Lett. 94, 251111 (2009).

[11] Chakravarty, S., Topol'ancik, J., Bhattacharya, P., Chakrabarti, S., Kang, Y. and Meyerhoff, M. E., "Ion detection with photonic crystal microcavities," Opt. Lett. 30, 2578 (2005).

[12] Sünner, T., Stichel, T., Kwon, S.H., Schlereth, T. W., Höfling, S., Kamp, M. and Forchel, A., "Photonic crystal cavity based gas sensor," Appl. Phys. Lett. 92, 261112 (2008).

[13] Kita, S., Nozaki, K. and Baba, T., "Refractive index sensing utilizing a cw photonic crystal nanolaser and its array configuration," Opt. Express 16, 8174 (2008).

[14] Kim, S., Lee, J., Jeon, H. and Kim, H. J., "Fiber-coupled surface-emitting photonic crystal band edge laser for biochemical sensor applications," Appl. Phys. Lett. 94, 133503 (2009).

[15] P. B. Deotare, M. W. McCutcheon, I. W. Frank, M. Khan, and M. Lončar, "High quality factor photonic crystal nanobeam cavities," Appl. Phys. Lett. 94, 121106 (2009).

[16] Gong, Y. and Vučković, J., "Photonic crystal cavities in silicon dioxide," Appl. Phys. Lett. 96, 031107 (2010).

[17] Deotare, P. B., McCutcheon, M. W., Frank, I. W., Khan, M. and Lončar, M., "Coupled photonic crystal nanobeam cavities," Appl. Phys. Lett. 95, 031102 (2009).

[18] Frank, I. W., Deotare, P. B., McCutcheon, M. W. and Lončar, M., "Programmable photonic crystal nanobeam cavities," Opt. Express 18, 8705 (2010).

[19] Eichenfield, M., Camacho, R., Chan, J., Vahala, K. J. and Painter, O., "A picogram- and nanometre-scale photonic-crystal optomechanical cavity," Nature 459, 550 (2009).

[20] Zhang, Y., Khan, M., Huang, Y., Ryou, J. H., Deotare, P., Dupuis, R. and Lončar, M., "Photonic crystal nanobeam lasers," Appl. Phys. Lett. 97, 051104 (2010).

[21] Gong, Y., Ellis, B., Shambat, G., Sarmiento, T., Harris, J. S. and Vučković, J., "Nanobeam photonic crystal cavity quantum dot laser," Opt. Express 18, 8781 (2010).

[22] Almeida, V. R., Xu, Q., Barrios, C. A. and Lipson, M., "Guiding and confining light in void nanostructure," Opt. Lett. 29, 1209 (2004).

[23] Wang, B., Dündar, M. A., Nötzel, R., Karouta, F., He, S. and van der Heijden, R. W., "Photonic crystal slot nanobeam slow light waveguides for refractive index sensing," Appl. Phys. Lett. 97, 151105 (2010).

[24] Dündar, M. A., Ryckebosch, E. C. I., Nötzel, R., Karouta, F., van IJzendoorn, L. J. and van der Heijden, R. W., "Sensitivities of InGaAsP photonic crystal membrane nanocavities to hole refractive index," Opt. Express 18, 4049 (2010).

[25] Johnson, S. G. and Joannopoulos, J. D., "Block-iterative frequency-domain methods for Maxwell's equations in a planewave basis," Opt. Express 8, 173 (2001).

[26] Oskooi, A. F., Roundy, D., Ibanescu, M., Bermel, P., Joannopoulos, J. D. and Johnson, S. G., "Meep: A flexible free-software package for electromagnetic simulations by the FDTD method," Comput. Phys. Commun. 181, 687-702 (2010).
[27] Ferrier, L., Rojo-Romeo, P., Drouard, E., Letatre, X. and Viktorovitch, P., "Slow Bloch mode confinement in 2D photonic crystals for surface operating devices," Opt. Express16, 3136 (2008)
[28] Nötzel, R., Anantathanasarn, S., van Veldhoven, R. P. J., van Otten, F. W. M., Eijkemans, T. J., Trampert, A., Satpati, B., Barbarin, Y., Bente, E. A. J. M., Oei, Y. S., de Vries, T., Geluk, E. J., Smalbrugge, B., Smit, M. K. and Wolter, J. H., "Self Assembled InAs/InP Quantum Dots for Telecom Applications in the 1.55 μm Wavelength Range: Wavelength Tuning, Stacking, Polarization Control, and Lasing," Jpn. J. Appl. Phys., Part 1 45, 6544 (2006).
[29] F. Schneider, ed., Sugar Analysis-ICUMSA, (International Commission for Uniform Methods of Sugar Analysis, (ICUMSA), 1979, (ICUMSA), 2009).